Desalination and Water Treatment
www.deswater.com

doi: 10.5004/dwt.2021.27268

226 (2021) 184–196
June

Simultaneous removal of phosphate and nitrate from polluted water using Zr-alginate beads doped with green synthesized nano-CeO_2 and active carbon of *Epipremnum aureum* plant as an effective adsorbent

Wondwosen Kebede Biftu[a,b], Kunta Ravindhranath[a,*]

[a]*Department of Chemistry, KoneruLakshmaiah Education Foundation, Green Fields, Vaddeswaram-522 502, Guntur Dt., Andhra Pradesh, India; email: ravindhranath.kunta@gmail.com*
[b]*Ethiopian Radiation Protection Authority, Addis Ababa, Ethiopia, email: wondwosenkebesmart@gmail.com*

Received 11 September 2020; Accepted 20 March 2021

ABSTRACT

A composite material comprising of green synthesized nano-cerium oxide and active carbon prepared from the leaves of *Epipremnum aureum* plants immobilized in Zr-alginate beads is successfully investigated as an adsorbent for the simultaneous removal of 'phosphate and nitrate' from polluted water. Extraction conditions are optimized. X-ray diffraction, Fourier-transform infrared spectroscopy, field emission scanning electron microscopy and energy-dispersive X-ray spectroscopy studies are adopted for characterizing the sorbent. Sorption mechanisms are investigated using various adsorption isotherms and kinetic models. Thermodynamics parameters are evaluated. The data reveal the Freundlich isotherm model of adsorption, pseudo-second-order kinetics and spontaneity of the sorption process. Adsorption capacity is: 75.63 mg/g for phosphate and 66.92 mg/g for nitrate. The spent beads can be regenerated and reused. The method is applied for the removal of 'phosphate and nitrate' ions from real polluted water. The merit of this investigation is that $nCeO_2$ particles are synthesized via green routes and these particles in combination with an active carbon-embedded in Zr-alginate beads, have good adsorption capacities at neutral pH for the successful simultaneous removal of 'phosphate and nitrate' ions from real polluted water.

Keywords: $nCeO_2$; Zr-alginate beads; *Epipremnum aureum*; Activated carbon; Water remediation; Phosphate and nitrate

1. Introduction

Nitrate and phosphate are common contaminants in water bodies and are toxic when their concentrations are more than 50 ppm for nitrates [1] and 50 μg/L for phosphate respectively [2] as per WHO. Nitrate is the ultimate oxidation product of nitrogenous matter of organic impurities in water under aerobic conditions. It is generated through the nitrogen cycle from anthropogenic sources such as septic tanks, human refuses, turf grass, and agricultural residues [3,4]. Further, nitrates find their way to water bodies due to over-fertilizing activities in agricultural fields. The main sources of phosphate pollution are agricultural run-offs, industrial sewages and domestic sewage wastes. Further, phosphate rocks weathering, human and animal excreta and food residues also contribute to phosphate pollution. Removal of nitrates and phosphates from polluted water is the most challenging environmental problem [5–7].

Consumption of nitrates contaminated water causes methamoglobinemia or blue babies. Nitrates and phosphates

* Corresponding author.

through the process of 'eutrophication' in lakes cause the loss of ecological balance in aquatic life. Due to the overgrowth of biota in lakes, dissolved oxygen content in water decreases, resulting in stress on aquatic life [8–10]. Hence, investigations are carried out to remove these ions from polluted water. On perusal of the literature, it is revealed that the removed phosphate and nitrate are affected based on physical, chemical and biological techniques [11–13] such as electrocoagulation [14], degradation [15] and fermentation [16]. The simultaneous removal of nitrate and phosphate using an effective adsorbent is a less trodden research concept. The present investigation endeavors to this endpoint.

Methods based on adsorption using plant based-materials as adsorbents are interesting to the researchers as the procedures are simple, effective and economical. These bio-sorbents are eco-friendly and synthesized from renewable bio-sources [17,18]. Recently, increasing findings are reported to purify water using adsorbents based on nanoparticles. The nanoparticles due to their size and inherited quantum confinements are proving to be effective adsorbents. High adsorption capacities are reported with these nano-based adsorbents [19,20]. Hence, in this work, we tried to develop an adsorbent based on active carbon and $nCeO_2$ particles synthesized via green routes. The composite material of 'active carbon and $nCeO_2$' is immobilized in Zr-alginate beads to impart better compatibility and easy filtration besides added adsorption nature of Zr-alginate beads. These beads are found to be effective in the simultaneous removal of 'nitrate and phosphate' at pH: 7 with good adsorption capacities. This finding is interesting as the adsorbent can be directly applied to polluted water without adjusting the pHs.

In the present work, the conditions for the maximum simultaneous removal of 'nitrate and phosphate' using 'Zr-alginate beads doped with $nCeO_2$ and active carbon' as adsorbent, are investigated and optimized. X-ray diffraction (XRD), Fourier-transform infrared spectroscopy (FTIR), field emission scanning electron microscopy (FESEM) and energy-dispersive X-ray spectroscopy (EDX) studies are employed for characterization. The nature of adsorption is analyzed by adopting different adsorption isotherms and kinetics models. Thermo-dynamical investigations are also made. The method developed is applied for the simultaneous removal of 'nitrate and phosphate' in synthetic mixers and also to the samples collected in polluted lakes in West Godavari District of Andhra Pradesh, India.

2. Materials and method

2.1. Reagents and chemicals

The chemicals used were of A.R. grade. Simulated solutions of nitrate, phosphate and other reagents were prepared with double-distilled water.

2.2. Active carbon generation

2.2.1. Plant

Epipremnum aureum is a house plant that belongs to the Arum family (Fig. 1). It grows well in tropical and subtropical conditions throughout the world.

2.2.2. Active carbon

Epipremnum aureum plant leaves were cut, washed with distilled water and dried under sunlight for 2 d. These dried leaves were immersed in concentrated H_2SO_4 for 24 h in a round-bottomed flask. Then the bio-material was digested for 3 h with condenser set-up. The bio-material was completely carbonized. Thus obtained biochar was filtered through G-3 crucibles and washed with distilled water repetitively for its neutrality. The biochar was dried at 105°C for 2 h in hot air-over. The biochar was crushed and sieved to the size: <75 μm. Thus activated biochar is named as ACLEA as per the terms 'activated carbon derived from leaves of *Epipremnum aureum*'.

2.2.3. Sapindus plant seeds skin extract

The hot water extract of skins of seeds of *Sapindus* plant was used as capping and stabilizing agent as described in our previous work [21].

2.3. Nano-CeO_2 synthesis

The requisite amount of $(NH_4)_2Ce(NO_3)_6$ was dissolved in a solvent's blend of 'water: ethylene glycol (4:1)' to obtain a solution of 0.05 N concentration. 100 mL of this cerium salt solution was taken into a 250 mL beaker and to which, 25.0 mL of extract of skins of *Sapindus* plant seeds was added and the resulting solution was stirred using a magnetic stirrer for 15 min. Then 5.0 g of urea was added and the solution was gradually heated while stirring until the solution had reached a temperature of 90°C. The precipitating agent, ammonia, was liberated due to urea hydrolysis and the pH of the solution was gradually increased. When the pH reached 9, the heating was stopped but stirring was continued for 10 h. This process of the homogeneous method of slow liberation of the precipitating agent prevented the super-saturation at local points and further, the increase in viscosity of the mother liquid by adding ethylene glycol prevents the fast growth of the nuclei of the hydroxides of Ce. These conditions helped the particles to grow slowly and when the particle reached nano-size, the natural capping agent (extract) prevented further growth. Thus obtained material was centrifuged, washed with distilled water until the pH of the filtrate was neutral and dried at 105°C for 2 h and calcinated in the muffled furnace for 6 h at 500°C. Then the material was cooled and preserved in sealed bottles.

2.4. Preparation of composite (CeO_2@ACLEA)

2.0 g of ACLEA and 1.0 g of nano-CeO_2 were taken into a 250 mL beaker. To this mixture, 100 mL of distilled water was added and stirred continuously at temperature: 80°C for a period of 4 h. The resulting solution was cooled to room temperature, filtered, washed with distilled water and dried at 105°C for 3 h in the oven. The composite was named as: $nCeO_2$@ACLEA (nano-cerium oxide loaded active carbon derived from leaves of *Epipremnum aureum*).

2.5. Zirconium alginate beads doped with CeO_2@ACLEA

2.5% w/v sodium alginate solution in distilled water was subjected to heating at 80°C to obtain a gel. 2.5 g of

Fig. 1. *Epipremnum aureum* plant.

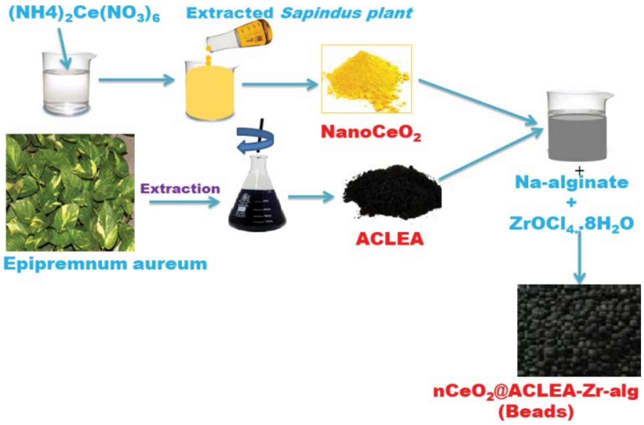

Fig. 2. Methodology for preparation of nCeO$_2$@ACLEA-Zr-Alg – beads.

'CeO$_2$@ACLEA' was added to the gel in small amounts through stirring for 3 h to get a homogeneous solution. The solution was cooled to room temperature and was added to 5°C cooled zirconyl chloride solution (taken in beaker), drop by drop with the help of a uniform bored-dropper. Beads doped with the composite material were formed and they were digested with the mother-liquor for 24 h at room temperature to facilitate the complete development of the beads. Thus resulted beads were filtered, washed with distilled water and dried at 80°C for 3 h. The beads were named as: nCeO$_2$@ACLEA-Zr-Alg as per the terms: zirconium alginate beads doped with 'nano-CeO$_2$ loaded ACLEA'. The methodology adopted for the synthesis is presented graphically in Fig. 2.

2.6. Extraction experiments

Batch modes of adsorption studies were employed [22–24]. Optimum conditions of extractions were investigated with individual simulated solutions of nitrate and phosphate. After establishing the conditions, the developed method was applied to the admixtures of synthetic simulated solutions of 'nitrate and phosphate'.

2.6.1. Establishment of optimum extraction conditions

For individual ions: known amounts of nitrate and phosphate were taken into 250 mL conical flasks and initial pHs were adjusted with dil. HCl or NaOH. The flasks were agitated in an orbital shaker for a desired period at 300 rpm and at temperature: 30°C ± 1°C. After required periods of equilibration, the solutions were filtered and the filtrates were analyzed using spectrophotometric methods as described in the literature [25]. Nitrate by sulphanilamide method and phosphate by molybdenum blue method was adopted.

% removals of NO_3^- and PO_4^{3-} and adsorption capacities of 'nCeO$_2$@ACLEA-Zr-Alg' (q_e) for the said anions, were evaluated by using equations [26,27].

$$\%\text{removal} = \frac{\left(C_0 - C_i\right)}{C_0} \times 100 \tag{1}$$

$$q_e = \frac{\left(C_0 - C_i\right)}{m} V \tag{2}$$

where C_0 and C_i are the initial and final concentrations (mg/L), m = mass of adsorbent (g); V = volume of the solution (L) of NO_3^- and PO_4^{3-}.

The effect of pH, 'nCeO$_2$@ACLEA-Zr-Alg'-dosage, time of contact, initial concentration of adsorbate, the effect of interfering ions, the temperature on the adsorptivities of the adsorbent were investigated. Regeneration and reuse of the spent adsorbent was also investigated. In assessing adsorptivities, the targeted parameter was gradually varied while all other experimental conditions were kept at optimum levels.

2.6.2. Analysis of mixtures of ions

The investigations carried in this work revealed that maximum removal of 'nitrate and phosphate' was possible at pH: 7 with 'nCeO$_2$@ACLEA-Zr-Alg' as adsorbent. For assessing whether the optimum conditions established for individual ions are good enough for the mixtures, investigations were made with the mixtures of nitrate and phosphate at the optimum conditions established with the individual ions. The results show that the adsorbent dosage is to be increased to 0.24 g/100 mL and time of equilibration to 60 min for the simultaneous removal of 'phosphate and nitrate'. Except for these minor changes in the parameters, the other extraction conditions are the same for individual ions as well as for the mixtures. The conditions of extractions and results of the adsorptive investigations for the removal of toxic nitrate and phosphate are presented in Table 1.

2.7. Characterization of 'nCeO$_2$@ACLEA-Zr-Alg'

The adsorbent was subjected to XRD, FTIR, EDX and FESEM studies. For this investigation, the spectrum or images of 'nCeO$_2$@ACLEA-Zr-Alg' were recorded before and after the adsorption of the adsorbates. The results are presented in Figs. 3–5.

Table 1
Simultaneous removal of nitrate and phosphate (optimum conditions: pH: 7; adsorbent dosage: 0.24 g/100 mL; time of equilibration: 60 min; rpm: 300; temp.: 30°C ± 1°C)

Simulated solution	Composition[a]				% Removal	
	Before adsorption		After adsorption			
	PO_4^{3-}	NO_3^-	PO_4^{3-}	NO_3^-	PO_4^{3-}	NO_3^-
1	10.0	25.0	0.09	1.95	99.10	92.2
2	15.0	30.0	1.005	2.97	93.3	90.1
3	20.0	40.0	1.64	5.08	91.8	87.3
4	25.0	50.0	2.375	7.5	90.5	85.0
5	30.0	60.0	3.06	9.96	89.8	83.4

[a]Average of five estimations; SD: ±0.20.

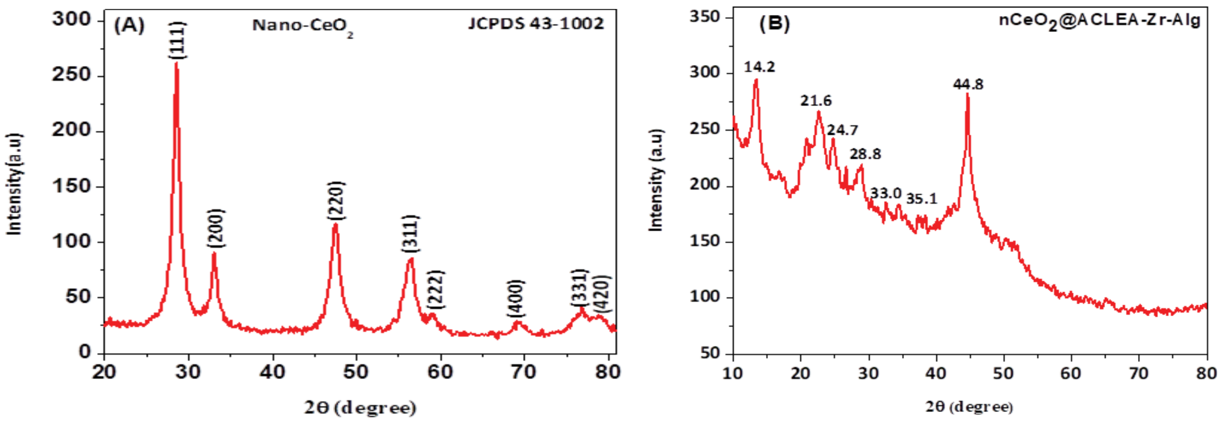

Fig. 3. XRD spectra of: (A) CeO_2 nanoparticles and (B) $nCeO_2$@ACLEA-Zr-Alg′.

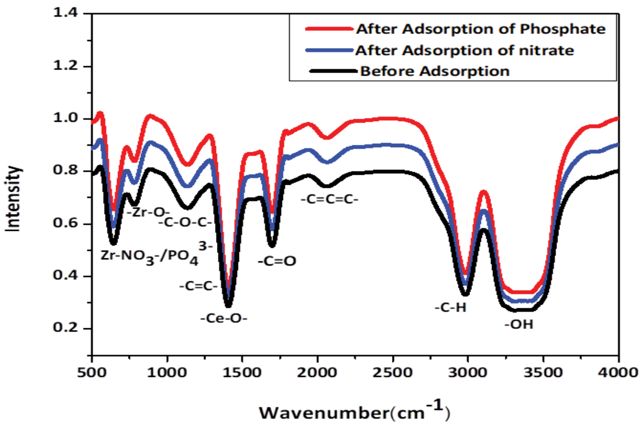

Fig. 4. FTIR spectra of before and after adsorption of NO_3^- and PO_4^{3-} ions.

2.8. Applications

The methodology developed was applied to treat lake waters from West Godavari District, Andhra Pradesh, India. The water bodies in this district were reported to be polluted with nitrate and phosphate due to intensive agricultural activities. The samples were analyzed for the existing nitrate and phosphate concentration levels. Then these samples were subjected to the treatment with the procedures developed in this work. The results are presented in Table 5.

3. Result and discussion

3.1. Characterization studies

3.1.1. XRD analysis

The observed XRD spectra for the green synthesized $nCeO_2$ and beads are presented in Fig. 3. The spectrum of $nCeO_2$ exhibited a series of well-defined peaks of CeO_2 at 2θ = 28.5°, 33.0°, 47.5°, 56.3°, 59.1°, 69.4°, 76.8° and 79.1°, which may be accounted for the diffractions of the (111), (200), (220), (311), (222), (400), (331), and (420) crystalline planes of face centered cubic (FCC) CeO_2, respectively as per JCPDS 43-1002.

The XRD spectrum of beads shows mixed peaks of active carbon, $nCeO_2$ and Zr-alginate. The strong diffraction peaks at 2θ = 24.8° and 2θ = 44.8° pertain to the active carbon, indicating the existence of graphite crystallite [29]. The two typical crystalline peaks of at 14.30° and 21.30° belong to zirconium alginate related to the crystal planes (4 2 2) and (5 1 1) respectively [30]. The peaks at 2θ = 28.5° and 33.0° may be attributed to $nCeO_2$ due

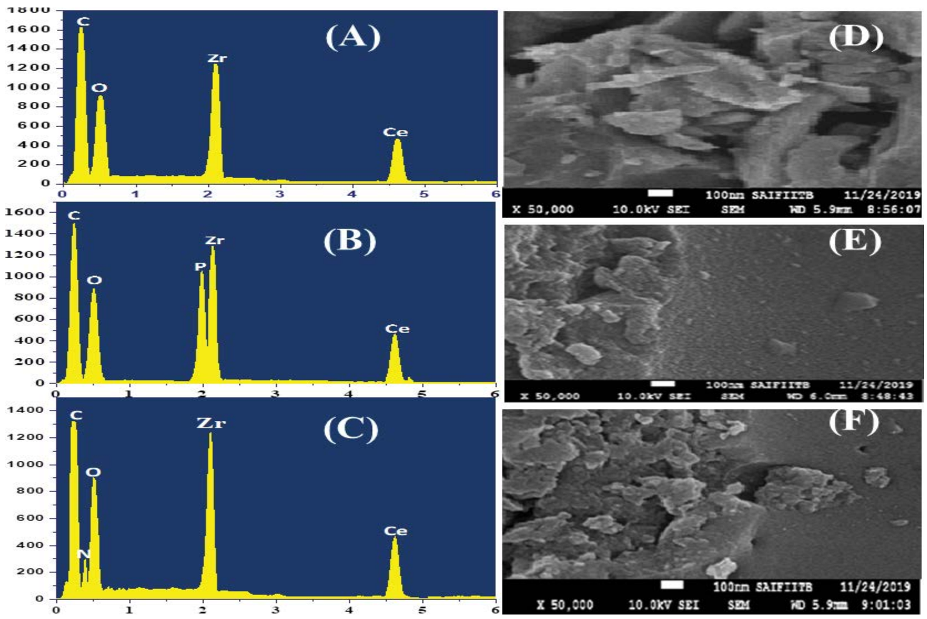

Fig. 5. EDX: (A) before, (B and C) after adsorption of PO_4^{3-} and NO_3^-; FESEM: (D) before, (E and F) after adsorption of PO_4^{3-} and NO_3^-.

to the diffraction at the planes (1 1 1) and (2 0 0) respectively [31]. Further, the XRD peak of $ZrO(OH)_2$ is noted at 35.55 [32]. The particle size of $nCeO_2$ was evaluated using the Scherrer formula [28].

$$L = \frac{k\lambda}{B\cos\theta} \tag{3}$$

where λ = radiation wavelength; B = physical width of a reflection (in 2θ); θ = diffraction angle of a line maximum; and K is a constant of value ≈ 0.9. The $nCeO_2$ particle size was found to be between 8.0 to 9.0 nm with an average size of 8.44 nm.

3.1.2. Fourier-transform infrared spectroscopy analysis

The FTIR spectra '$nCeO_2$@ACLEA-Zr-Alg'-before and after adsorption of 'phosphate and nitrate' are presented in Fig. 4. The absorption band observed at ~3,350 cm^{-1} in the spectrum of adsorbent pertains to the stretching vibrations of the '–OH' group. This frequency is shifted to 3,355 cm^{-1} after adsorption of NO_3^- and to 3,358 cm^{-1} after PO_4^{3-} adsorption. The frequency at 2,972 cm^{-1} in before adsorption spectrum is due to stretching of 'C–H' groups. It is shifted to 2,975 and 2,982.3 cm^{-1} after the adsorption of nitrates and phosphate respectively. The frequency at 2,055 cm^{-1} attributed to the allene (C=C=C) group is shifted to 2,060 and 2,065 cm^{-1} after the adsorption of nitrate and phosphate respectively.

The frequency at 1,700 cm^{-1} attributed to C=O is shifted to 1,705 cm^{-1} after NO_3^- adsorption and 1,710 cm^{-1} after PO_4^{3-} adsorption. The strong absorption band at 1,408.5 cm^{-1} before adsorption, 1,412 cm^{-1} after adsorption of NO_3^- and 1,415 cm^{-1} after PO_4^{3-} adsorption is attributed to stretching vibrations of C=C and '–Ce–O–PO_4^{3-}/NO_3^-. The sharp bands at 1,130 cm^{-1} (before adsorption) are due to 'C–O–C' stretching vibrations and it is shifted to 1,132 and 1,135 cm^{-1} after adsorption of nitrate and phosphate respectively. A sharp small peak at 778 cm^{-1} before adsorption pertains to Zr–O (stretching) is shifted to 780 and 785 cm^{-1} after adsorption of nitrate and phosphate respectively. The frequency at 638.5 cm^{-1} before adsorption and the frequencies at 640.5 and 645.3 cm^{-1} after adsorption of nitrate and phosphate respectively, are due to asymmetric stretching of 'Zr-PO_4^{3-}/NO_3^-. The changes in the peak positions and intensities indicate that there are interactions between nitrate and phosphate with the functional groups of '$nCeO_2$@ACLEA-Zr-Alg'.

3.1.3. Energy-dispersive X-ray spectroscopy

The EDX spectra of adsorbent '$nCeO_2$@ACLEA-Zr-Alg'-before and after adsorption of NO_3^- and PO_4^{3-}, are presented in Figs. 5A–C. In comparison of the spectra, it is evident that peaks pertaining to N and P are appeared in the spectrum taken after adsorption (Figs. 5B and C). These peaks are missing in the before adsorption spectrum (Fig. 5A). These features are emphatic proofs for the adsorption NO_3^- and PO_4^{3-} by '$nCeO_2$@ACLEA-Zr-Alg'-beads.

3.1.4. FESEM analysis

FESEM of '$nCeO_2$@ACLEA-Zr-Alg'taken before and after adsorption of nitrate and phosphate are presented in Figs. 5D–F. Rough, micropores, spongy, irregular and heterogeneous structures can be noted in the before adsorptions image (Fig. 5D). In the images take after adsorption of nitrate and phosphate, there are marked changes in the images: missing pores or decrease in pore size, and disappearance of some corners and edges (Figs. 5E and F). These features reflect that the adsorption of NO_3^- and PO_4^{3-} onto the surface of the adsorbent.

3.2. Factors influencing the adsorptivity

Various extraction conditions were investigated to assess their effect on the adsoptivities of the adsorbent for nitrate and phosphate.

3.2.1. Effect of pH

The effect of pH of the equilibrating solution on the adsorptivity of adsorbent for 'phosphate and nitrate' was assessed by varying the pH from 2.0 to 12.0 but keeping all other parameters at constant values. The results are presented in Fig. 6A. The maximum removal of 96.6% for phosphate and 94.5% for nitrate are observed at neutral pH: 7 below and above this pH, the % removal is decreased. This is an important finding as it facilitates the simultaneous removal of 'nitrate and phosphate' and moreover at neutral pH.

From Fig. 6B, pH_{zero} for 'nCeO$_2$@ACLEA-Zr-Alg' was evaluated as: 7.0. At this pH, the surface of the adsorbent is neutral and above and below this value, the surface is charged. At the optimum pH: 7, phosphate ($H_2PO_4^-$ and HPO_4^{2-}) and nitrate (NO_3^-) exist as anions. Hence, the adsorption of nitrate and phosphate at neutral conditions cannot be due to electrostatic interactions. So, the adsorption of nitrate and phosphate may be due to a short of complex formation between the said ions and adsorbent functional groups. This is supported by the thermodynamic data evaluated for the adsorption process in this investigation.

3.2.2. Effect of sorbent concentration

By changing the sorbent dosage from 0.08 to 0.14 g/100 mL but maintaining other extraction conditions at constant levels, % removal was investigated. The results are depicted in Fig. 6C. The adsorption of 'phosphate and nitrate' is increased linearly with an increase in the concentration of adsorbent initially. But it has reached a steady-state after a certain concentration of the adsorbent. The maximum extraction is: 96.6% for phosphate with 0.12 g/100 mL; and 94.5% for nitrate with 0.13 g/100 mL. With the increase in the dosage of the adsorbent, naturally, the number of adsorption sites available for the adsorption process increases and hence, more adsorption is observed initially. But when the adsorbent is further increased, the proportional increase in adsorption is not observed. This may be due to the blocking of pathways for adsorbates to reach the active sites laid in the matrix of the adsorbent due to aggregation and/or deposition.

3.2.3. Effect of time

Agitation time is the time allowed for equilibration between adsorbates and adsorbents. The optimum time needed for maximum removal of nitrate and phosphate was investigated by estimating the % removal at varied time intervals of equilibration. The results are presented in Fig. 6D. The adsorption is rapid initially and is slow down with the progress of time and attained steady state after 40 min for phosphate and 50 min for nitrate. Initially, the availability of active sites is more and so, the rate of adsorption is more. With time, the active sites are used up and hence, the adsorption rate is decreased. As the quantity of the adsorbent is fixed: 0.12 g/100 mL for phosphate and 0.13 g/100 mL nitrate, the active sites are fixed. When all the sites are engaged with the adsorption of adsorbates, steady states have resulted.

3.2.4. Effect of initial concentration

The initial concentration of adsorbate is another important parameter that influences the adsorption process. So, the effect of various initial concentrations of phosphate and nitrate on the % removal was investigated and the results are depicted in Figs. 6E and F. With the increase of concentration from 10 to 150 mg/L, % removal is decreased from 96.6% to 52.5% for PO_4^{3-} and 94.5% to 49.5% for NO_3^- (Fig. 6E). As the sorbent dosage is fixed only a fixed number of active sites are available. So, as the concentration of adsorbate is increased, the number of available 'active sites per ion' is decreased and hence, % removal falls. However, the adsorption capacity (q_e) is increasing with the increase in the concentration of adsorbate, Fig. 6F. As the concentration is increased from 10 to 150 mg/L, the values of q_e are increased from 8.05 to 75.63 mg/g for PO_4^{3-} and 7.23 to 66.92 mg/g for NO_3^-. This may be attributed to the fact that as the concentration of nitrate and phosphate is increased, the concentration gradient between the bulk of the solution and the surface of the adsorbent with respect to the adsorbate is also increased. This causes the adsorbates to diffuse more towards the surface of the adsorbent and thereby resulting in more adsorptivities.

3.2.5. Effect of temperature

The effect of solution temperature on the adsorptivities of 'nCeO$_2$@ACLEA-Zr-Alg' for phosphate and nitrate was investigated. The findings are noted in Figs. 6G and H. Adsorptivity is increased with an increase in temperature. An increase in solution temperature enhances the vibrational kinetic energy of the functional groups present on the surface of 'nCeO$_2$@ACLEA-Zr-Alg' and thereby decreases the surface-layer thickness. Further, the adsorbate ions acquire more kinetic energy. These two factors help in the penetration of adsorbate deeper into the 'nCeO$_2$@ ACLEA-Zr-Alg' and hence, more adsorptivities with an increase in temperature.

3.3. Simultaneous removal of phosphate and nitrate

From Section 3.2, it may be inferred that the phosphate and nitrate are removed to an extent of 96.6% and 94.5% respectively at pH: 7 from the 10 mg/L concentration of the adsorbate at the optimum conditions: equilibration time: 40 min for phosphate and 50 min for nitrate; dosage of 'nCeO$_2$@ACLEA-Zr-Alg: 0.12 g/100 mL for phosphate and 0.13 g/100 mL for nitrate; rpm: 300; and temperature: 30°C ± 1°C. Thus at pH:7, the simultaneous removal of phosphate and nitrate was investigated by changing the sorbent dosage from 0.2 g/100 mL to 0.28 g/100 mL and time of equilibration from 10 to 90 min. The other extraction conditions are maintained at optimum levels as evaluated for individual ions.

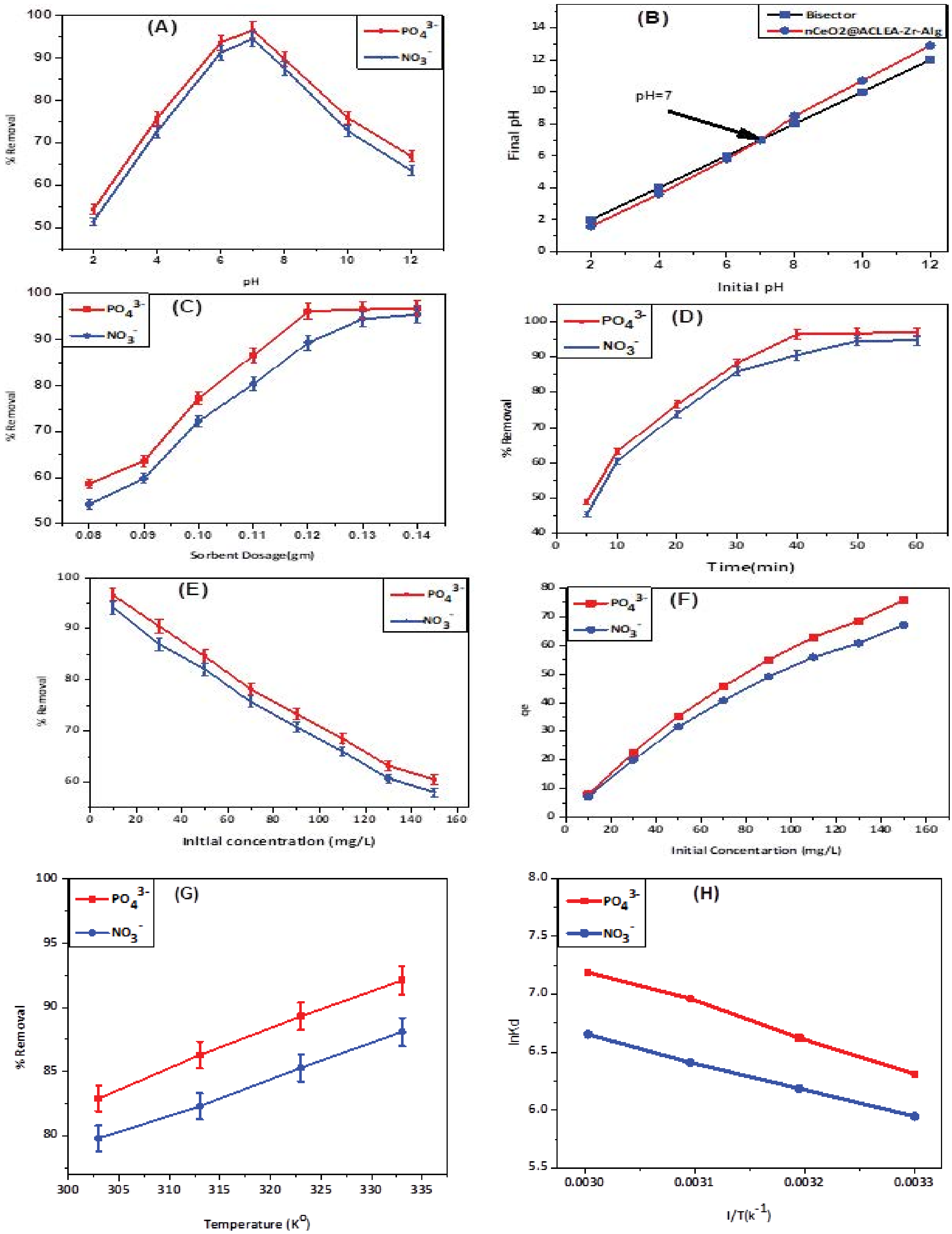

Fig. 6. (A) Effect of pH, (B) evaluation of pH_{zpc}, (C) effect of dosage, (D) effect of contact time, (E) effect of initial concentrations, (F) adsorption capacities, q_e vs. initial concentration, (G and H) effect of temperature.

For this, simulated solutions having admixtures of nitrate and phosphate in different proportions as noted in Table 1, were prepared and subjected to the extraction with the adsorbent: $nCeO_2$@ACLEA-Zr-Alg, at the optimum conditions established in this study. The results are noted in Table 1. It may be inferred from the table that substantial amounts of nitrate and phosphate can be simultaneously removed at the convenient neutral pH: 7.

3.3.1. Thermodynamic studies

The sign and magnitude of thermodynamic properties namely, Gibbs free energy (ΔG), entropy (ΔS), and enthalpy (ΔH) provide insight into the strength and type of bonds between adsorbate and adsorbent. These factors were evaluated using the following equations.

$$\Delta G = \Delta H - T\Delta S \tag{4}$$

$$\Delta G = -RT \ln K_d \tag{5}$$

$$\ln K_d = \frac{\Delta S}{R} - \frac{\Delta H}{RT} \tag{6}$$

where q_e = amount of adsorbed adsorbate, K_d = distribution coefficient of the adsorption, R = gas constant, and T = thermodynamic temperature in Kelvin as described in the literature [33,34]. The results are presented in Table 2.

Negative ΔG values reflect the spontaneity and endothermic nature of the adsorption process. The negative values are increasing as the temperature increases. This indicates more favorable conditions of adsorption at elevated temperatures. Change in enthalpy (ΔH) values was 25.96 kJ/mol for PO_4^{3-} and 23.45 kJ/mol for NO_3^-. The magnitudes of the values indicate the chemical nature of the adsorption process. A sort of surface complex formation occurs between the adsorbate and the functional groups of the sorbent, $nCeO_2$@ACLEA-Zr-Alg.

Positive ΔS values and their magnitudes are the testimony of disorder at the 'solid/liquid' interface. As the disorder is more, the chances of adsorbate ions to cross over the boundary between the solution and solid-adsorbent, is more and hence, more adsorptivities.

3.4. Adsorption nature

The adsorption mechanism was analyzed using various isotherm models. The Freundlich, Eq. (1) [35], Langmuir, Eq. (2) [36], Temkin, Eq. (3) [37], and Dubinin–Radushkevich, Eq. (4) [38], isothermal models were employed to understand the adsorption mechanisms as described in the literature [39,40]. The pertaining equations used are:

$$\log(q_e) = \log k_F + \left(\frac{1}{n}\right)\log C_e \tag{7}$$

$$\left(\frac{C_e}{q_e}\right) = \left(\frac{a_L}{k_L}\right)C_e + \frac{1}{k_L} \tag{8}$$

$$q_e = B\ln C_e + B\ln A \tag{9}$$

$$\ln q_e = -\beta\varepsilon^2 + \ln q_m \tag{10}$$

In Figs. 7A–D and Table 3, the pertaining results are presented. It can be inferred from the correlation coefficient (R^2) that the Freundlich adsorption model having higher correlation coefficients: R^2 = 0.992 for nitrate and 0.994 for phosphate, describe well the adsorption nature. This indicates the heterogeneous and multi-layer adsorption at the surface of '$nCeO_2$@ACLEA-Zr-Alg'. Further, the Langmuir adsorption model of R_L values was found to be 0.465 for nitrate and 0.523 for phosphate. As per Hall et al. [41], these values imply the favourability of the adsorption process. From Temkin and Dubinin–Radushkevich equations 'E and B' values are evaluated and presented in Table 3.

3.5. Kinetics of adsorption

Pseudo-first-order [18,42], pseudo-second-order [43,44], Bangham's pore diffusion model [45,46] and Elovich model [47], were employed in analysing the kinetics of adsorption. The pertaining evaluated factors are depicted in Table 4. From Table 4, it may be inferred that the $R2$ values fall in the order: pseudo-second-order > Elovich > pseudo-first-order > Bangham's pore diffusion.

The data of NO_3^- and PO_4^{3-} are better modeled by pseudo-second-order rate kinetics (as in Fig. 8) as their correlation coefficients (R^2) are 0.996 for PO_4^{3-} and 0.998 for NO_3^- as compared to the other rate models. So, the pseudo-second-order model describes well the adsorption process.

3.6. Co-ions interference

The effect of a two-fold excess of co-ions naturally found in water on % removal of nitrate and phosphate was investigated. Results are presented in Fig. 9. From the data, it may be inferred that the cations namely, Mg^{2+}, Ca^{2+}, Fe^{2+},

Table 2
Evaluation of thermodynamics parameters

Adsorbate	ΔH (kJ/mol)	ΔS (kJ/mol)	ΔG (kJ/mol)				R^2
			303°K	313°K	323°K	333°K	
PO_4^{3-}	25.96	134.9	–15.41	–16.55	–17.69	–18.83	0.99
NO_3^-	23.45	114.04	–13.37	–14.35	–15.32	–16.29	0.99

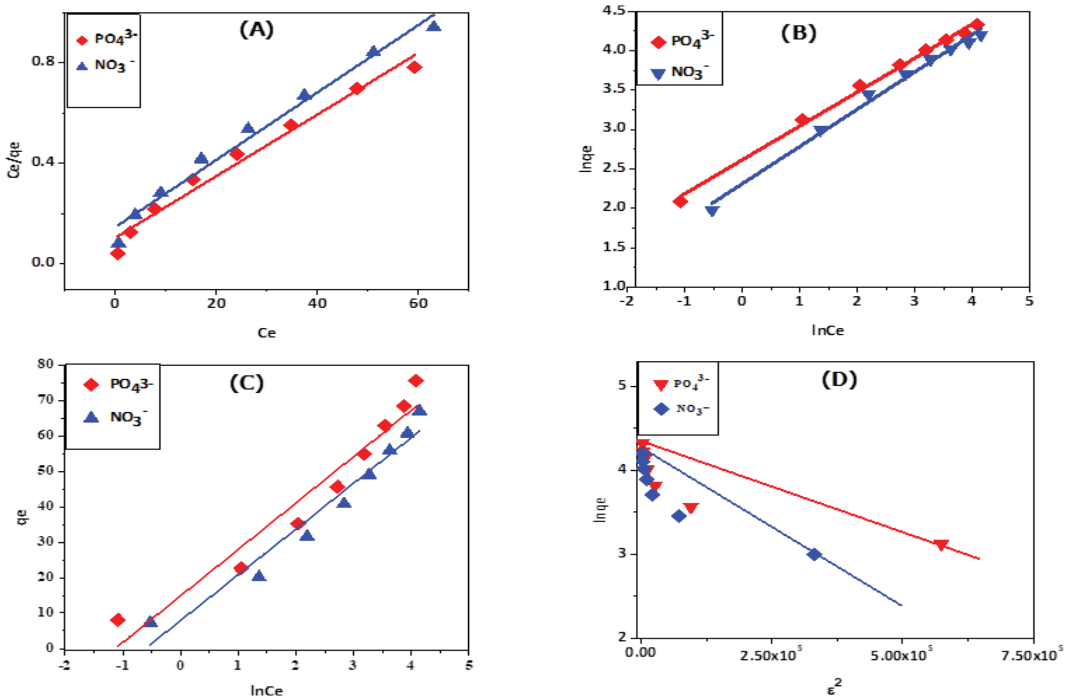

Fig. 7. Adsorption isotherm models: (A) Langmuir, (B) Freundlich, (C) Temkin and (D) Dubinin–Radushkevich.

Table 3
Assessed adsorption isothermal parameters

Adsorbate		Langmuir isotherm	Freundlich isotherm	Temkin isotherm	Dubinin–Radushkevich isotherm
Phosphate	Slope	0.0134	0.473	13.12	–1.55E-07
	Intercept	0.147	2.62	14.85	3.9
	R^2	0.979	0.994	0.933	0.718
		R_L = 0.523	$1/n$ = 0.0134	B = 13.12	E = 1.8 kJ/mol
Nitrate	Slope	0.0122	0.43	12.92	–2.97E-07
	Intercept	0.106	2.32	7.88	3.79
	R^2	0.974	0.992	0.946	0.722
		R_L = 0.465	$1/n$ = 0.0122	B = 12.92	E = 1.3 kJ/mol

Zn^{2+} and anions: Cl^-, CO_3^{2-}, F^- are marginally interfered. SO_4^{2-} has shown some interference.

3.7. Regeneration and reuse

Regeneration of spent adsorbents by treating with suitable eluents and their subsequent use as adsorbents is one of the important aspects. This recycling helps to decrease the cost of the treatment process. Hence, in this work many eluents comprising acids, bases and salts were investigated for the regeneration of the spent 'nCeO$_2$@ACLEA-Zr-Alg'. It was observed that 0.01 N NaOH was effective in restoring the adsorption capacity of the spent 'nCeO$_2$@ACLEA-Zr-Alg'. The findings are presented in Fig. 10. The beads structure of the adsorbent has not deteriorated and was robust enough even after five regenerations. % remove of PO_4^{3-} and NO_3^- and even with 5th regenerated 'nCeO$_2$@ACLEA-Zr-Alg' is 88.4% and 86.30% respectively. Moreover, the repeated use of the regenerated adsorbent can remove completely PO_4^{3-} and NO_3^- ions from polluted water.

3.8. Applications

In this investigation, the developed nCeO$_2$@ACLEA-Zr-Alg was applied to treat polluted lake water samples collected from West Godavari District, Andhra Pradesh, India. Due to intensive agricultural activities and over-use of fertilizers, the water bodies of this area were reportedly polluted with respect to nitrate and phosphate. The collected samples from West Godavari District, Andhra Pradesh, India were analyzed for the existing concentrations of nitrate and phosphate and cited in Table 5. The samples from the Lake water were subjected to treatment with nCeO$_2$@ACLEA-Zr-Alg for the simultaneous removal of 'nitrate and phosphate' at pH: 7 with the sorbent dosage: 0.24 g/100 mL; time of equilibration: 60 min; rpm; 300; and temperature

30°C ± 1°C. The results are presented in Table 1. It is revealed from the table that the $nCeO_2$@ACLEA-Zr-Alg is very effective in the treatment of water for the removal of nitrate and phosphate.

3.9. Comparison with previous works

The present developed adsorbent, $nCeO_2$@ACLEA-Zr-Alg is compared with different good adsorbents based on bio-materials and nano-materials reported, so far, for the removal of PO_4^{3-} and NO_3^-. These adsorbents are compared with respect to pH and adsorbent capacities. The data is presented in Table 6. It can be observed that $nCeO_2$@ACLEA-Zr-Alg is more effective than many of the adsorbents reported. Further, the present investigation permits the simultaneous removal of 'nitrate and phosphate' at the comfortable neutral pH:7.

Table 4
Assessed characteristics for kinetic models

		Phosphate	Nitrate
Pseudo-first-order model	R^2	0.978	0.975
	Intercept	0.75	0.68
	Slope	–0.0297	–0.129
Pseudo-second-order model	R^2	0.996	0.998
	Intercept	0.77	0.93
	Slope	0.12	0.121
Elovich model	R^2	0.98	0.979
	Intercept	0.96	1.3
	Slope	1.6	1.73
Bangham's pore diffusion	R^2	0.974	0.972
	Intercept	–1.89	–1.85
	Slope	0.313	0.297

4. Conclusions

Nano-cerium oxide particles are successfully synthesized by green methods. These particles are admixed with an active carbon prepared by digesting leaves of the *Epipremnum aureum* plant in hot H_2SO_4. Thus obtained composite comprising of $nCeO_2$ and active carbon are immobilized in Zr-alginate beads. These beads are investigated as adsorbents for the removal of nitrate and phosphate. Optimum extraction conditions are established. The beads show maximum adsorption for nitrate and phosphate at neutral pH: 7. This feature enables the establishment of the procedure for the simultaneous removal of nitrate and phosphate from water. XRD, FTIR, FESEM and EDX techniques are used in characterizing the adsorbent and adsorption process.

Adsorption nature is investigated using various adsorption isotherms, kinetic models and thermodynamics studies. The data reveals the Freundlich isotherm model of adsorption, pseudo-second-order kinetics and spontaneity

Table 5
Applications

Samples	Initial concentration of ions, C_i^a (mg/L)		Concentration of ions after treatment, C_e^a (mg/L)		% Removal[a]	
	NO_3^-	PO_4^{3-}	NO_3^-	PO_4^{3-}	NO_3^-	PO_4^{3-}
1	5.4	1.8	0	0	100	100
2	12.7	2.2	0	0	100	100
3	18.4	2.6	0.81	0.03	95.6	98.7
4	25.1	3.4	2.13	0.17	91.5	95.1
5	34.2	4.1	3.8	0.35	88.9	91.5

[a]Average of five determinations; SD: ±0.15.

Table 6
Comparison with reported good adsorbents in literature

S. No.	Adsorbent	pH	Names of ions	Uptake capacity (mg/g)	Reference
1	3D graphene–La_2O_3 composite	6.2	Phosphate	82.6	[48]
2	Activated carbon residue	4	Nitrate	3.8	[49]
3	NH_4^+ functionalized meso-SiO_2	8	Nitrate	46.0	[50]
4	Fe–Ti nanocomposite	6.8	Phosphate	35.4	[51]
5	Chitosan/zeolite/$nCeO_2$	6	Nitrate	23.58	[52]
6	La–Zr/peel	6.2	Phosphate	40.21	[53]
7	Nano-alumina	4.4	Nitrate	4.0	[54]
8	Nano-Ag@ACTR	3	Phosphate	13.62	[55]
9	$nCeO_2$@ACLEA-Zr-Alg	7	Phosphate	75.625	This study
10	$nCeO_2$@ACLEA-Zr-Alg	7	Nitrate	66.92	

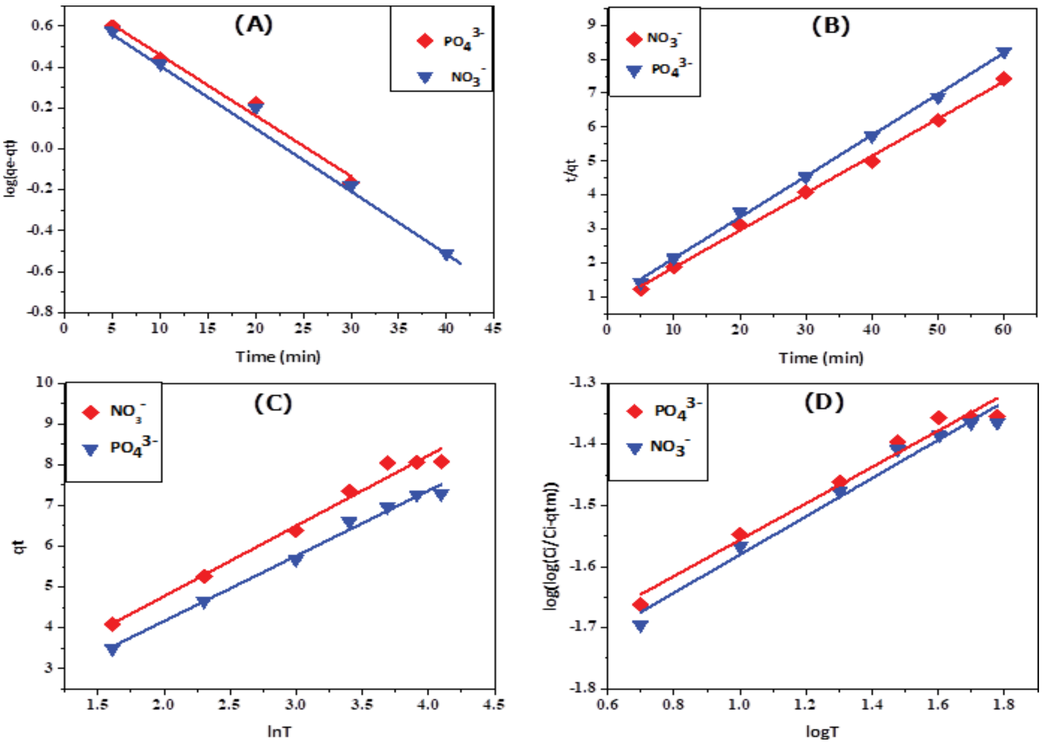

Fig. 8. Adsorption kinetics: (A) pseudo-first-order kinetics, (B) pseudo-second-order kinetics, (C) Elovich model, and (D) Bangham's pore diffusion model.

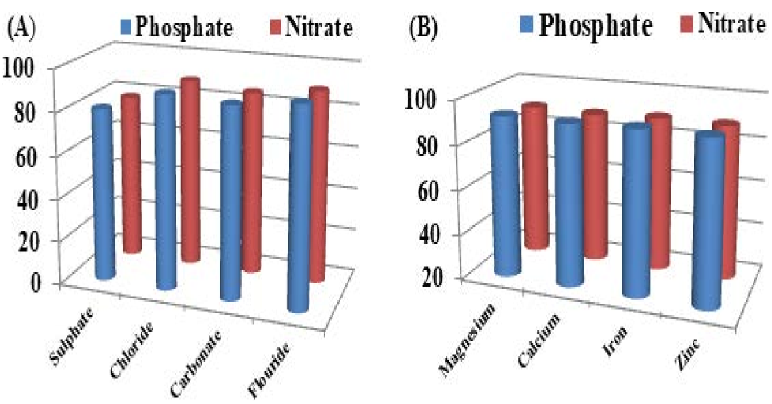

Fig. 9. Effect of interfering co-anions and co-cations, on % removal of phosphate and nitrate ions.

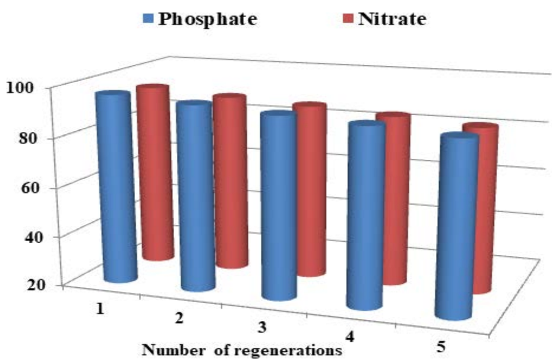

Fig. 10. Number of regenerations vs. % removal.

of the sorption process. Maximum adsorption capacity is 75.63 mg/g for phosphate and 66.92 mg/g for nitrate. The spent beads can be regenerated and reused. The method is used for the simultaneous removal of 'phosphate and nitrate' ions from real polluted water.

References

[1] Z.H. Shen, X.Y. Dong, J.L. Shi, Y.H. Ma, D.R. Liu, J. Fan, Simultaneous removal of nitrate/phosphate with bimetallic nanoparticles of Fe coupled with copper or nickel supported on chelating resin, Environ. Sci. Pollut. Res., 26 (2019) 16568–16576.

[2] H. Seresht, E.Z. Afsharian, M.E. Bidhendi, H.R. Nodeh, M.A. Kamboh, M. Yilmaz, Removal of phosphate and nitrate

ions aqueous using strontium magnetic graphene oxide nanocomposite: isotherms, kinetics, and thermodynamics studies, Environ. Prog. Sustainable Energy, 39 (2020) e13332, doi: 10.1002/ep.13332.
[3] R. Sadler, B. Maetam, B. Edokpolo, D. Connell, J. Yu, D. Stewart, M.-J. Park, D. Gray, B. Laksono, Health risk assessment for exposure to nitrate in drinking water from village wells in Semarang, Indonesia, Environ. Pollut., 216 (2016) 738–745.
[4] L.T. Stayner, K. Almberg, R. Jones, J. Graber, M. Pedersen, M. Turyk, Atrazine and nitrate in drinking water and the risk of preterm delivery and low birth weight in four Midwestern states, Environ. Res., 152 (2017) 294–303.
[5] A. Sowmya, S. Meenakshi, Effective utilization of the functional groups in chitosan by loading Zn(II) for the removal of nitrate and phosphate, Desal. Water Treat., 54 (2015) 1674–1683.
[6] E. Bock, M. Smith, B. Rogers, B. Coleman, M. Reiter, B. Benham, Z.M. Easton, Enhanced nitrate and phosphate removal in a denitrifying bioreactor with biochar, J. Environ. Qual., 44 (2015) 605–613.
[7] F. Ogata, A. Ueda, S. Tanei, D. Imai, N. Kawasaki, Simultaneous removal of phosphate and nitrite ions from aqueous solutions using modified soybean waste, J. Ind. Eng. Chem., 35 (2016) 287–294.
[8] J. Zolgharnein, K. Dalvand, M. Rastgordani, P. Zolgharnein, Adsorptive removal of phosphate using nano cobalt hydroxide as a sorbent from aqueous solution; multivariate optimization and adsorption characterization, J. Alloys Compd., 725 (2017) 1006–1017.
[9] E.M. Zong, G.B. Huang, X.H. Liu, W.W. Lei, S.T. Jiang, Z.Q. Ma, J.F. Wang, P.G. Song, A lignin-based nano-adsorbent for superfast and highly selective removal of phosphate, J. Mater. Chem., A, 6 (2018) 9971–9983.
[10] L. Wang, J.Y. Wang, C. He, W. Lyu, W.L. Zhang W. Yan, L. Yang, Development of rare earth element doped magnetic biochars with enhanced phosphate adsorption performance, Colloids Surf., A, 561 (2019) 236–243.
[11] W.T. Mook, M.H. Chakrabarti, M.K. Aroua, G.M.A. Khan, B.S. Ali, M.S. Islam, M.A. Abu Hassan, Removal of total ammonia nitrogen (TAN), nitrate and total organic carbon (TOC) from aquaculture wastewater using electrochemical technology: a review, Desalination, 285 (2012) 1–13.
[12] F. Aloui, S. Kchaou, S. Sayadi, Physicochemical treatments of anionic surfactants wastewater: effect on aerobic biodegradability, J. Hazard. Mater., 164 (2009) 353–359.
[13] A. Rezaee, M. Safari, H. Hossini, Bioelectrochemical denitrification using carbon felt/multiwall carbon nanotube, Environ. Technol., 36 (2015) 1057–1062.
[14] Y. Tian, W. He, X. Zhu, W. Yang, N.Q. Ren, B.E. Logan, Improved electrocoagulation reactor for rapid removal of phosphate from wastewater, ACS Sustainable Chem. Eng., 5 (2017) 67–71.
[15] Z.F. Ma, Y. Yang, Y.H. Jiang, B.D. Xi, X.Y. Lian, Y.N. Xu, Effects of anions on bio-chemical degradation of nitrate in groundwater, Environ. Earth Sci., 74 (2015) 3985–3992.
[16] Y. Yuan, J.J. Liu, B. Ma, Y. Liu, B. Wang, Y.Z. Peng, Improving municipal wastewater nitrogen and phosphorous removal by feeding sludge fermentation products to sequencing batch reactor (SBR), Bioresour. Technol., 222 (2016) 326–334.
[17] A.N. Babu, G.V.K. Mohan, K. Ravindhranath, Removal of chromium(VI) from polluted waters using adsorbents derived from *Chenopodium album* and *Eclipta prostrate* plant materials, Int. J. ChemTech Res., 9 (2016) 506–516.
[18] S. Ravulapalli, R. Kunta, Enhanced removal of chromium(VI) from wastewater using active carbon derived from *Lantana camara* plant as adsorbent, Water Sci. Technol., 78 (2018) 1377–1389.
[19] K. Ravindhranath, M. Ramamoorty, Nano aluminum oxides as adsorbents in water remediation methods: a review, Rasayan J. Chem., 10 (2017) 716–722.
[20] W.K. Biftu, K. Ravindhranath, M. Ramamoorty, New research trends in the processing and applications of iron-based nanoparticles as adsorbents in water remediation methods, Nanotechnol. Environ. Eng., 5 (2020) 1–12, doi: 10.1007/s41204-020-00076-y.
[21] W.K. Biftu, K. Ravindhranath, Synthesis of nanoZrO_2 via simple new green routes and its effective application as adsorbent in phosphate remediation of water with or without immobilization in Al-alginate beads, Water Sci. Technol., 81 (2020a) 2617–2633.
[22] R.K. Trivedy, Pollution Management in Industries, Environmental Publications, 2nd ed., Karad, India, 1995.
[23] R. Sujitha, K. Ravindhranath, Effective removal of methylene blue, a hazardous dye from industrial effluents using active carbon of F.infectoria plant, Int. J. Environ. Sci. Technol., 16 (2019) 7837–7848.
[24] A.N. Babu, G.V.K. Mohan, K. Kalpana, K. Ravindhranath, Removal of fluoride from water using H_2O_2-treated fine red mud doped in Zn-alginate beads as adsorbent, J. Environ. Chem. Eng., 6 (2018a) 906–916.
[25] APHA, Standard Methods for the Examination of Water and Waste Water, American Public Health Association, Washington, DC, 1985.
[26] W.T. Cai, F.L. Fu, L.J. Zhu, B. Tang, Simultaneous removal of chromium(VI) and phosphate from water using easily separable magnetite/pyrite nanocomposite, J. Alloys Compd., 803 (2019) 118–125.
[27] S. Ravulapalli,K. Ravindhranath, Novel adsorbents possessing cumulative sorption nature evoked from Al_2O_3 nanoflakes, C.urens seeds active carbon and calcium alginate beads for defluoridation studies, J. Taiwan Inst. Chem. Eng., 101 (2019) 50–63.
[28] G.A. Dorofeev, A.N. Streletskii, I.V. Povstugar, A.V. Protasov, E.P. Elsukov, Determination of nanoparticle sizes, Colloid J., 74 (2012) 710–720.
[29] Z.G. Xie, W. Guan, F.Y. Ji, Z.R. Song, Y.L. Zhao, Production of biologically activated carbon from orange peel and landfill leachate subsequent treatment technology, J. Chem., 2014 (2014) 491912 (1–9), doi: 10.1155/2014/491912.
[30] X.H. Zhao, Q. Li, X.M. Ma, Z. Xiong, F.Y. Quan, Y.Z. Xia, Alginate fibers embedded with silver nanoparticles as efficient catalysts for reduction of 4-nitrophenol, RSC Adv., 5 (2015) 49534–49540.
[31] W.K. Biftu, R. Kunta, Iron-alginate beads doped with green synthesised 'nano-CeO_2-ZrO_2' as an effective adsorbent for removal of highly toxic arsenic-ions from polluted water, Int. J. Environ. Anal. Chem., (2021) 1875452 (1–19), doi: 10.1080/03067319.2021.1875452.
[32] H. Cui, Q. Li, S. Gao, J.K. Shang, Strong adsorption of arsenic species by amorphous zirconium oxide nanoparticles, J. Ind. Eng. Chem., 18 (2012) 1418–1427.
[33] T. Jin, W.H. Yuan, Y.J. Xue, H. Wei, C.Y. Zhang, K. Li, Co-modified MCM-41 as an effective adsorbent for levofloxacin removal from aqueous solution: optimization of process parameters, isotherm, and thermodynamic studies, Environ. Sci. Pollut. Res., 24 (2017) 5238–5248.
[34] A.N. Babu, G.V.K. Mohan, K. Kalpana, K. Ravindhranath, Removal of lead from water using calcium alginate beads doped with hydrazine sulphate-activated red mud as adsorbent, J. Anal. Methods Chem., 2017 (2017) 4650594 (1–13), doi: 10.1155/2017/4650594.
[35] H.M.F. Freundlich, Over the adsorption in solution, J. Phys. Chem., 57 (1906) 1100–1107.
[36] I. Langmuir, The adsorption of gases on plane surfaces of glass, mica and platinum, J. Am. Chem. Soc., 40 (1918) 1361–1403.
[37] M.J. Temkin, V. Pyzhev, Recent modifications to Langmuir isotherms, Acta Phys. USSR, 12 (1940) 217–222.
[38] M.M. Dubinin, L.V. Radushkevich, The equation of the characteristic curve of activated charcoal, Proc. Acad. Sci. Phys. Chem. Sect. USSR, 55 (1947) 331–333.
[39] A.N. Babu, D.S. Reddy, G.S. Kumar, K. Ravindhranath, G.V.K. Mohan, Removal of lead and fluoride from contaminated water using exhausted coffee grounds based bio-sorbent, J. Environ. Manage., 218 (2018) 602–612.
[40] S. Ravulapalli, K. Ravindhranath, Removal of lead(II) from wastewater using active carbon of *Caryota urens* seeds and its embedded calcium alginate beads as adsorbents, J. Environ. Chem. Eng., 6 (2018a) 4298–4309.
[41] K.R. Hall, L.C. Eagleton, A. Acrivos, T. Vermeulen, Pore- and solid-diffusion kinetics in fixed-bed adsorption under

constant-pattern conditions, Ind. Eng. Chem. Fundam., 5 (1966) 212–223.
[42] J.F. Corbett, Pseudo-first-order kinetics, J. Chem. Educ., 49 (1972) 663.
[43] Y.S. Ho, G. McKay, Pseudo-second-order model for sorption processes, Process Biochem., 34 (1999) 451–465.
[44] W.K. Biftu, S. Ravulapalli, R. Kunta, Effective de-fluoridation of water using *Leucaena luecocephala* active carbon as adsorbent, Int. J. Environ. Res., 14 (2020b) 415–426.
[45] Y.S. Ho, J.C.Y. Ng, G. McKay, Kinetics of pollutant sorption by biosorbents: review, Sep. Purif. Rev., 29 (2000) 189–232.
[46] G.K. Mohan, A.N. Babu, K. Kalpana, K. Ravindhranath, Removal of chromium(VI) from water using adsorbent derived from spent coffee grounds, Int. J. Environ. Sci. Technol., 16 (2019) 101–112.
[47] F.-C. Wu, R.-L. Tseng, R.-S. Juang, Characteristics of Elovich equation used for the analysis of adsorption kinetics in dye-chitosan systems, Chem. Eng. J., 150 (2009) 366–373.
[48] M.L. Chen, C.B. Huo, Y.K. Li, J.H. Wang, Selective adsorption and efficient removal of phosphate from aqueous medium with graphene–lanthanum composite, ACS Sustainable Chem. Eng., 4 (2016) 1296–1302.
[49] S. Kilpimaa, H. Runtti, T. Kangas, U. Lassi, T. Kuokkanen, Physical activation of carbon residue from biomass gasification: novel sorbent for the removal of phosphates and nitrates from aqueous solution, J. Ind. Eng. Chem., 21 (2015) 1354–1364.
[50] S. Hamoudi, R. Saad, K. Belkacemi, Adsorptive removal of phosphate and nitrate anions from aqueous solutions using ammonium-functionalized mesoporous silica, Ind. Eng. Chem. Res., 46 (2007) 8806–8812.
[51] J.B. Lu, D.F. Liu, J. Hao, G.W. Zhang, B. Lu, Phosphate removal from aqueous solutions by a nano-structured Fe–Ti bimetal oxide sorbent, Chem. Eng. Res. Des., 93 (2005) 652–661.
[52] A. Teimouri, S.G. Nasab, N. Vahdatpoor, S. Habibollahi, H. Salavati, A.N. Chermahini, Chitosan/zeolite Y/Nano ZrO_2 nanocomposite as an adsorbent for the removal of nitrate from the aqueous solution, Int. J. Biol. Macromol., 93 (2016) 254–266.
[53] A. Muhammad, X. Xu, B.Y. Gao, Q.Y. Yue, Y. Shang, R. Khan, A.I. Muhammad, Adsorptive removal of phosphate by the bimetallic hydroxide nanocomposites embedded in pomegranate peel, J. Environ. Sci., 91 (2020) 189–198.
[54] A. Bhatnagar, E. Kumar, M. Sillanpää, Nitrate removal from water by nano-alumina: characterization and sorption studies, Chem. Eng. J., 163 (2010) 317–323.
[55] V.T. Trinh, T.M.P. Nguyen, H.T. Van, L.P. Hoang, T.V. Nguyen, L.T. Ha, X.H. Vu, T.T. Pham, T.N. Nguyen, N.V. Quang, X.C. Nguyen, Phosphate adsorption by silver nanoparticles-loaded activated carbon derived from tea residue, Sci. Rep., 10 (2020) 36334 (1–13), doi: 10.1038/s41598-020-60542-0.